https://doi.org/10.48048/tis.2025.9119

Enhanced Photocatalytic Degradation of Congo Red Dye Using Green-Synthesized TiO_2 and PANI/TiO_2 with Papaya Leaf as Bio-Reduction

Nugrahani Primary Putri*, Agus Mifthakhul Riska, Diah Hari Kusumawati and Evi Suaebah

Department Physics, Universitas Negeri Surabaya, Jawa Timur 60213, Indonesia

(*Corresponding author's e-mail: nugrahaniprimary@unesa.ac.id)

Received: 11 October 2024, Revised: 24 October 2024, Accepted: 1 November 2024, Published: 20 November 2024

Abstract

This study uses the green synthesis method to investigate the photocatalytic properties of TiO_2 nanoparticles (NPs) and PANI/TiO2 nanocomposites (NCs). The in-situ polymerization method used the papaya leaf extract as a reducing agent. TiO_2 NPs have a particle size of 56 nm and a band gap of 2.46 eV, while PANI/TiO_2 NCs have a particle size of 44 nm and a band gap of 2.06 eV. The performance of TiO_2 NPs and PANI/TiO_2 NCs as semiconductor-based photocatalysis was evaluated using Congo red dye degradation. The results showed that PANI/TiO_2 NCs have better photocatalytic performance with a Congo red dye degradation rate of 97.12 %, higher than TiO_2 nanoparticles (95.52 %). This enhanced performance can contribute to the synergistic effect between the TiO_2 and PANI, leading to improved charge separation and reduced recombination.

Keywords: Photocatalysis, TiO_2 NPs, PANI/TiO_2 NCs, Degradation

Introduction

Water is an essential natural resource for life, but human activities endanger water supply systems. Industrial activities released many heavy metal ions, hazardous organic contaminants, aromatic phenols, industrial materials, and pharmaceuticals into surface waters, causing widespread water pollution [1]. There are more than 10,000 types of synthetic dyes that are still used commercially, with a total annual production of almost 800,000 tons [2]. Textile waste has intense colors that, even in low concentrations, can block light from entering the water [3]. This causes severe problems for aquatic ecosystems and organisms, such as photosynthesis disorders, organism death, and increased ammonia, which impacts human health [4]. Congo red is a synthetic red dye with an azo group (-N=N-) often dissolved in industrial waste and cannot be naturally decomposed. Therefore, removing this dye from water and waste is essential [5]. Many methods and technologies were used to treat wastewater, such as membranes, coagulation/flocculation, ozone treatment, ion exchange, biological and chemical oxidation, adsorption, and photocatalysis [6]. Photocatalysis is recognized as a promising method due to its flexibility, ease of operation, simplicity of design, and ability to remove pollutants and dyes effectively [7]. Potential photocatalytic materials for photodegradation are semiconductor materials, such as nickel metal oxide (NiO), titanium dioxide (TiO_2), zinc oxide (ZnO), magnesium oxide (MgO), and copper oxide (CuO), which have stable and safe characteristics [8].

Titanium dioxide (TiO_2) has become a material of great interest in materials science and chemistry due to its unique properties [9]. TiO_2 is an ideal photocatalyst because it has high chemical and thermal stability, is not easily decomposed by chemical reactions or temperature changes, has a long service life, and is non-toxic and environmentally friendly [10]. TiO_2 can degrade organic and inorganic pollutants in water and waste, producing cleaner water. However, conventional TiO_2 synthesis uses hazardous and toxic chemicals like sulfuric acid and hydrogen peroxide. This causes the TiO_2 synthesis process to be environmentally unfriendly and has the potential to cause negative impacts on human health and the environment. Papaya leaves as reducing agents were introduced by Kaur, and the result reported that synthesizing TiO_2 using the green synthesis method was successful [11].

To optimize the recombination of electron (e^-) - hole (h^+) pairs, most researchers have used conductive polymers to modify TiO_2 to improve electron transfer performance, such as polypyrrole/ TiO_2, polyaniline/TiO_2 and polythiophene/ TiO_2 [12]. Of the many polymers, polyaniline (PANI) is a conducting polymer that has become one of the centers of attention for academic and industrial communities to be studied. This polymer is easy to make, affordable, has good thermal stability, can offer a large surface area, and its properties can be easily manipulated with reversibility of doping-dedoping [6]; it consists of a comprehensive π-conjugated electron system expressing insolubility and stability in aqueous media [13]. Polyaniline has ion exchange properties and can remove pollutants from aqueous solutions, including heavy metals and dyes. The ion exchange properties of this polymer depend on different conditions, including polymerization conditions, the presence of stabilizers, the type of dopants, and the size of the polymer [14]. PANI has semiconductor properties with high conductivity, allowing efficient charge transfer. PANI also has superior redox properties and can expand the photocatalyst's surface by providing more active sites, thus increasing photocatalytic performance [15]. The PANI/RGO nanocomposites have better dye degradation capacity than just PANI or RGO [16]. Another result shows that PANI/SnO_2 nanocomposites have excellent dye removal efficiency compared to pure SnO_2, and the preparation of Ag-ZnO/PANI nanocomposites showed excellent dye removal efficiency compared to Ag-ZnO nanoparticles [17].

Incorporating metal oxides with polymers improves the efficiency and effectiveness of photocatalysis. TiO_2 has a low surface area that limits the active sites for photocatalytic reactions. Adding polymer (PANI) increases the surface area, provides more active sites for solution adsorption and degradation, and acts as an excellent adsorbent material [18]. The polymer stabilizes TiO_2 nanoparticles, prevents agglomeration, maintains their activity, and facilitates the separation of TiO_2 from water for reuse. In addition, the polymer can act as an electron conductor, enhancing the charge transfer between TiO_2 and the substrate and improving photocatalysis efficiency [19].

Based on the information from the research results above, the application of TiO_2 nanoparticles combined with PANI has never been reported on the degradation of Congo red dye, so this study has a novelty in the application of TiO_2 nanoparticles using the green synthesis method from papaya leaves (*Carica Papaya L.*) combined with PANI to degrade Congo red dye with the hope that the presence of PANI in the TiO_2 compound, the photocatalytic process can run faster and more effectively. This supports the achievement of the 6^{th} Sustainable Development Goals (SDGs), namely clean water and sanitation, which aims to ensure the availability and management of clean water and sustainable sanitation for all because the technology discussed in this study can help to increase access to clean water, maintain the quality of clean water, and protect the environment [20].

Materials and methods

Green synthesis TiO_2 NPs

Papaya leaves (*Carica Papaya L.*) were collected and washed with running water to remove dirt on the surface, and then the clean leaves were chopped. The leaves were dried at 55 °C in an oven (Faithul FCE-3000 Serials) for 180 min. The dried leaves were blended on a beaker glass (Herma), and the powder obtained was stored. Papaya leaf extract was obtained by mixing 10 g of papaya leaf powder with 100 mL of distilled water and stirring for 60 min at a temperature of 50 - 60 °C using a magnetic stirrer. The extract obtained after stirring and heating was filtered using filter paper for nanoparticle synthesis. TiO_2 nanoparticles were obtained using a magnetic stirrer by adding 40 mL of 0.5 M TTIP in 40 mL of extract with a 1:1 (v/v) ratio under continuous stirring at 650 rpm. After 30 min, 8 mL of ammonia was added dropwise to the mixture, and a precipitate was obtained. The precipitate was separated from the mixture by filtration and washed with ethanol to remove ions and other impurities. The washed precipitate was dried in an electric oven at 100 °C and then crushed using a mortar and pestle. The fine TiO_2 powder was calcined at 570 °C in a muffle furnace.

Synthesis of PANI/TiO_2 NCs

The in-situ polymerization method was used to synthesize PANI/TiO_2 composites by referring to Putri *et al.* [20] and Nazli Turkten *et al.* [10] research. 0.91 mL of 0.1 M aniline monomer was added to 1M HCl and stirred for 15 min. After that, 4.78 g of Titanium isopropoxide (TiO_2) (Sigma Aldrich, 97 %) was added slowly. Subsequently, 0.1 M ammonium peroxydisulfate (APS) was introduced via pipette while continuously stirring for 4 h. The solution was to stand for 12 h. Furthermore, a gray precipitate was produced, signifying the completion of polymerization. The precipitate was collected, filtered, and rinsed with distilled water and acetone 3 - 4 times, then heated in an oven at 80 °C for 16 h. The precipitate was crushed using a mortar to create a PANI/TiO_2 composite.

Characterization of TiO_2 NPs and PANI/TiO_2 NCs

X-ray Diffraction (XRD) characterization was used to determine the formation of primary phases in the sample. The type of XRD tool used is the Smartlab Rigaku brand equipped with High Score Plus software and PDF with the latest version, which has a Cu anode radiation source, 40 kV, 30 mA, with a CuKα wavelength of 1.54056Å and uses Bragg-Brentano optical rays, for crystal measurements using the following Scherrer Eq. (1):

$$D = \frac{\lambda K}{\beta \cos \theta} \tag{1}$$

Sample measurements used a test angle of 10 - 90 ° with a step size of 0.010/min, the Scherrer constant (K) is 0.89 and β is a measure of the width of a peak or distribution at half of its maximum height, so each peak has its own FWHM value. The sample's morphology was identified using an SEM (Scanning Electron Microscopy) tool with a magnification of 25,000 times with the Jeol JSM-IT200 type equipped with EDX (Energy Dispersive X-ray). Horiba Scientific tools were used in the PL (Photoluminescence Micro spectrometer) test to detect structural defects and the potential recombination rate in the sample. UV Vis was characterized using a Hitachi UH-5300 tool to measure the absorbance at a 200 - 800 nm wavelength. From these data, the band gap analysis can be done using the following Tauc-plot as shows in Eq. (2):

$$(\alpha h v)^{2} = D(hv - Eg) \tag{2}$$

Data from the test results, in the form of relationship graphs, were then plotted, and the results were matched with reference.

Photocatalytic activity

The photocatalytic application process begins with diluting the Congo red dye to match the desired concentration. A 100 mL solution of Congo red was mixed with 10 mg (0.01 g) of the catalyst and stirrer for 1 h. The stirred solution was then exposed to UV light (inserting the sample into the UV box) at 30, 60, 90, 120, 150, and 180 min intervals. The solution absorbance was measured using UV-Vis to determine the absorbance value. To determine the percentage of PANI/TiO_2 degradation, can use the following Eq. (3) [21]:

$$\%\ \text{Degradation} = \frac{Ao - At}{Ao} \times 100\ \% \tag{3}$$

where A_0 and A_t is the initial and final absorbance of Congo red after t min.

Results and discussion

Phase identification

With bio-reductants derived from papaya leaf extract (*Carica Papaya L.*), the green synthesis method has successfully produced TiO_2 NPs. White TiO_2 NPs powder was obtained after several stages of synthesis. The crystal structure of TiO_2 was identified using XRD (**Figure 1**, black curve). After analyzing the results of XRD characterization by matching with JCPDS card number 01-078-2486, it was found that the TiO_2 synthesis results had an Anatase phase [22]. The average size of TiO_2 crystallites was calculated using the Debye-Scherrer equation at 9.65 nm. This study has successfully synthesized PANI/TiO_2 composites using in-situ polymerization methods in addition to TiO_2 synthesis. The synthesis of gray PANI/TiO_2 is a combination of PANI (blackish green) and TiO_2 (white). In addition, the PANI/TiO_2 sample produced from the synthesis was also characterized by XRD to determine the crystal structure formed (**Figure 1**, red curve). The

XRD results of the PANI/TiO_2 composite showed that, when compared with the diffractogram of TiO_2 powder, it was seen that there was no clear peak in the PANI diffractogram (**Figure 1**, blue curve), which is a fact that PANI has an amorphous (non-crystalline) structure [23]. The average crystallite size of the PANI/TiO_2 composite was 9.81 nm after being calculated using the Debye Scherrer equation.

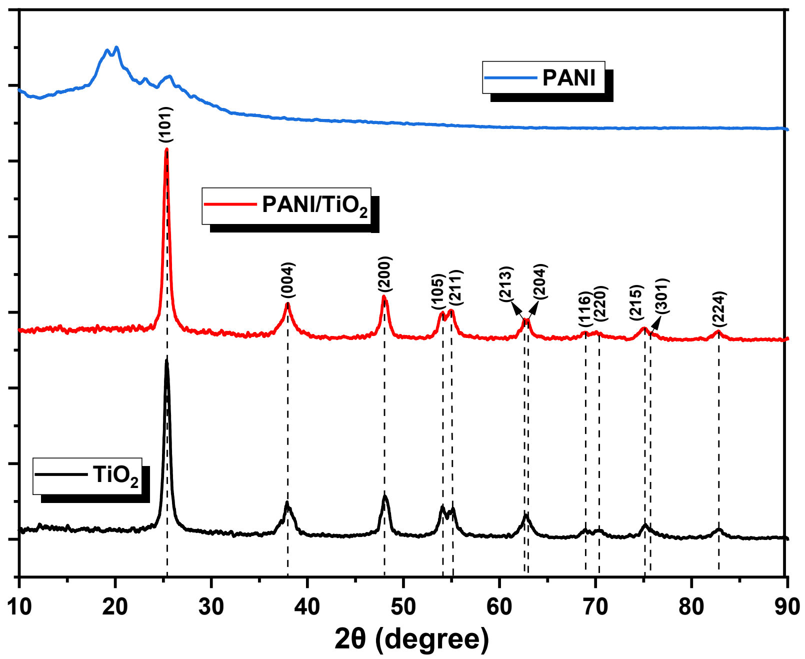

Figure 1 Phase identification results.

Morphological observation

Scanning Electron Microscopy and Energy Dispersive X-ray (SEM-EDX) characterization are used to determine the morphology of a material, identify the elements contained in the material, and analyze the chemical composition of the material. In this study, SEM magnification of 25,000x was used. The results of SEM characterization can be analyzed using ImageJ software to estimate the material's grain size. The morphology of PANI from oxidation polymerization was analyzed using SEM (**Figure 2(a)**). It is shown that the morphology of PANI is in the form of coral flowers in groups and has an average particle diameter of 81 nm. The EDX characterization results show that the elements contained in PANI are C, N, and O, which have the chemical formula $(C_5H_6NH_2)_n$.

Figure 2(b) shows the morphology of TiO_2 from green synthesis using papaya leaf extract bio reductor. Although some agglomerates exist, they are spherical and have fairly even distributions. In general, TiO_2 nanoparticles have a uniform size and shape distribution. The average particle size of TiO_2 nanoparticles was calculated using *ImageJ* software, as shown in **Figure 2(e)**. It was found that the average particle diameter was 56 nm, which means that this proves that TiO_2 is a nano-sized material [24]. The EDX identification results obtained several elements, including titanium (Ti), oxygen (O), carbon (C), and potassium (K). The observed C and K peaks were caused by ascorbic acid ($C_6H_8O_6$) and minerals (Ca, Mg, Na, K, Fe, and Mn) found in papaya leaf extract [25]. This analysis confirms that papaya leaves' content actively participates in the green synthesis of TiO_2. The results of the EDX analysis also confirm the high purity of TiO_2 from green synthesis because there are no impurities.

Figure 2(c) shows the PANI/TiO_2 composite has agglomerate morphology. This agglomeration is possible due to the interaction between PANI and TiO_2 materials, which causes both to agglomerate. On the other hand, this is the expected modification result because the PANI/TiO_2 material can be more stable during the photocatalytic application process. **Figure 2(f)** shows the average size of the PANi/TiO_2 NCs particle diameter, which is 44 nm. **Figure 2(i)** shows the peaks of titanium (Ti), oxygen (O), carbon (C), and nitrogen (N) elements and the corresponding atomic and weight percentages. In the EDX graph, the nitrogen element (N) is a typical PANI element that confirms the presence of PANI and indicates the success of the PANI/TiO_2 NCs material synthesis.

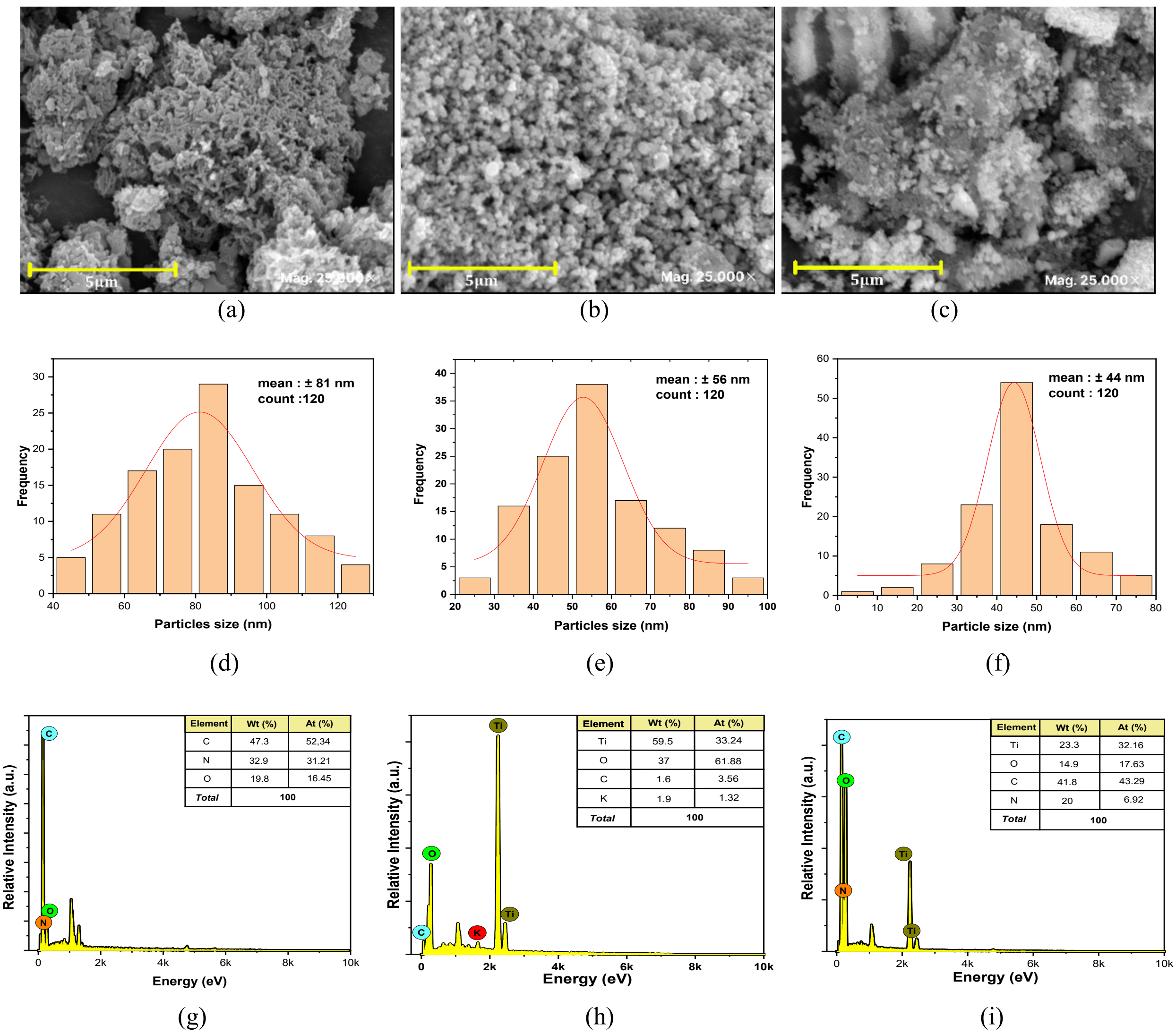

Figure 2 Observation Results (a) - (c) Morphology, (e) - (f) Quantitation of Particle Diameter Size and (g) - (i) Chemical Composition.

Determination of band gap energy value and optical properties of TiO_2 NPs and PANI/TiO_2 NCs

UV-Vis testing was carried out to determine the band gap energy value of TiO_2 NPs and PANI/TiO_2 NCs. The results obtained from the UV-Vis test are in the form of a wavelength spectrum and absorbance value. The UV Vis spectrum shows that the absorbance peak is at a wavelength of 303.69 nm for TiO_2 NPs and 349.01 nm for PANI/TiO_2 NCs. The band gap energy is the difference between the lower end of the valence band (+) and the upper end of the conduction band (−), known as the minimum energy required to excite electrons from the valence band to the conduction band. It can be calculated using the wavelength and absorbance values that have been obtained. The band gap value can be calculated using a linear graph of the relationship between E (eV) on the x-axis and ($\alpha h\upsilon$) on the y-axis, called the Tauc-plot method. Band gap energy is an essential factor affecting catalyst materials' effectiveness.

Based on the Tauc-plot equation, it was found that the band gap energy of TiO_2 NPs was 2.46 eV, while the band gap energy of PANI/TiO_2 NCs was 2.06 eV. These results indicate that both samples are ideal for photocatalytic applications [26]. They can function as effective photocatalyst materials because they intensively react when exposed to UV light and show better potential than other studies with band gap energy values [11]. PANI/TiO_2 NCs material is more practical because it has a smaller band gap energy. The smaller the band gap energy, the better the photocatalysis process because less energy is needed to push electrons from the valence band to the conduction band. Increased reaction efficiency due to electron

transfer from TiO_2 to PANI can achieve high catalytic activity because the energy band gap of PANI is lower than that of TiO_2.

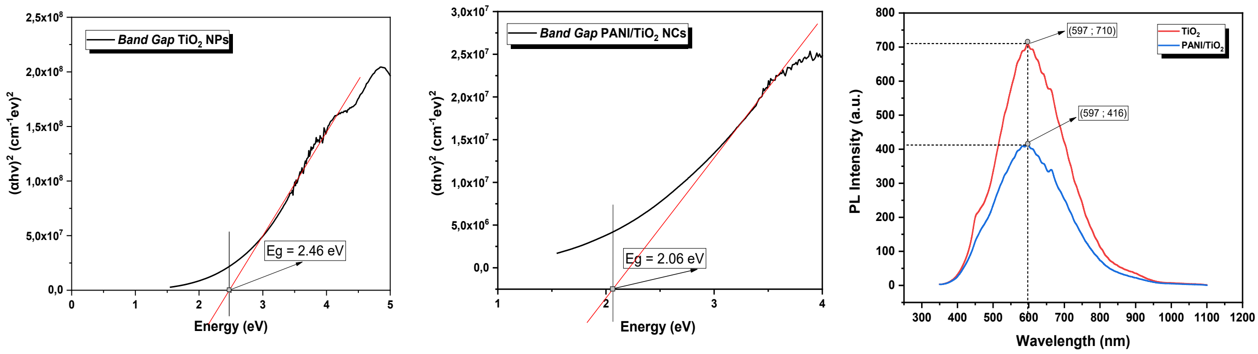

(a) (b) (c)

Figure 3 Determination of band gap energy (a) TiO_2 NPs (b) PANI/TiO_2NCs (c) Photoluminescence spectrum.

The optical properties of a material can be characterized by photoluminescence spectroscopy (PL) testing, which provides information related to the charge mobility of a material. The PL spectrum of TiO_2 NPs and PANI/TiO_2 NCs is presented in **Figure 3(c)**. PL emission occurs due to the radiative recombination of energetic electrons and holes, showing the emission results of the material at a wavelength of 597 nm for all samples; this indicates that TiO_2 NPs and PANI/TiO_2 semiconductors can be excited by photons with the appropriate energy to produce photogenerated electron and hole pairs [27]. The intensity of the TiO_2 NPs spectrum is higher than PANI/TiO_2 NCs. High catalytic activity can be achieved from increased reaction efficiency due to electron transfer from TiO_2 to PANI because the valence band edge of PANI has much lower energy than TiO_2. The weaker PL intensity of PANI/TiO_2 NCs may occur due to polyaniline trapped in the titania lattice. Therefore, the charge separation increases, and the radiative recombination decreases [28]. The results of this test indicate that incorporating PANI can improve the performance of nanocomposites by reducing the recombination rate, which makes the photocatalytic process more efficient compared to pure TiO_2 NPs, which is by previous studies [29].

Photocatalytic activity

The photocatalytic activity was conducted using a 40 ppm Congo red dye solution, with a catalyst mass of 10 mg (0.01 g) in 100 mL of solution, with 2 different catalyst materials, TiO_2 NPs, and PANI/TiO_2 NCs. The application was conducted by varying the time during the irradiation process for 30, 60, 90, 120, 150, and 180 min. The preparation was done by mixing 10 mg of catalyst into a 100 mL Congo red solution, stirring for 1 h using a magnetic stirrer in dark conditions and then continuing with the irradiation process using UV light. Each sample completed in the irradiation process was analyzed using UV-Vis spectroscopy to determine the absorbance value of the solution.

Figure 4 shows the absorbance results of the Congo red solution after irradiation for 180 min using TiO_2 NPs catalyst and PANI/TiO_2 NCs. The graph displaying the solution using the PANI/TiO_2 NCs catalyst demonstrates a more stable degradation compared to the graph of the solution using TiO_2 NPs. In this context, stability signifies that the reduction in absorbance occurs gradually within a relatively constant range for each decrement. In addition, the graph indicates that an increase in irradiation time correlates with a decrease in the absorbance value of the Congo red solution. Activating the catalyst by UV light emission improves the photocatalysis process and can take place. The photocatalytic process occurs when UV light excites electrons from the valence band to the conduction band of TiO_2 NPs. This leads to the formation of electron-hole excitation pairs in the conduction band and valence band. These pairs subsequently engage with water molecules, oxygen, and hydroxyl ions, forming reactive oxygen species such as superoxide radicals ($-O_2$) and free holes (h^+), highly reactive oxidative agents. These hydroxyl radicals can interact with complex dye compounds, leading to the degradation of complex chemical bonds and producing simpler compounds [30]. The concentration of the solution influences the absorbance value at 0 min (A_0); the higher the concentration of the solution, the higher the absorbance at A_0, and vice versa. Furthermore, this phenomenon is attributed to the increasing number of dye molecules, in which the amount of light (photon quantum) that penetrates the dye solution to reach the catalyst surface is reduced due to obstacles in the light path, which causes the absorbance value to increase.

Figure 4(c) illustrates the graph of the percentage of degradation of congo red solution at a concentration of 40 ppm by TiO_2 and PANI/TiO_2 catalysts. The graph indicates an increase in the irradiation time correlates with a higher degradation percentage. Moreover, the percentage of degradation value at the same application time (t) typically increases along with the concentration of congo red solution. The graph demonstrates that after 180 min of irradiation, the degradation percentage of the solution using PANI/TiO_2 NCs catalyst material is higher than using TiO_2 NPs catalyst, specifically 97.12 % compared to 95.52 %. The red graph is more linear than the black graph, indicating that degradation using PANI/TiO2 NCs catalyst is more stable than TiO_2 NPs catalyst. The maximum degradation percentage of PANI/TiO_2 NCs material is higher than TiO_2 NPs; this aligns with previous studies and research on degrading methylene blue dye [10]. These results are possible because the PANI/TiO_2 band gap value is smaller, causing less energy to excite electrons so that the photocatalytic process can run more effectively [30]. The photoluminescence intensity of PANI/TiO_2 NCs is lower than TiO_2 NPs, increasing the charge separation process (electrons and hole) and reducing radiative recombination due to the presence of polyaniline trapped in the titania lattice, thereby, the photocatalytic process can run more efficiently [27].

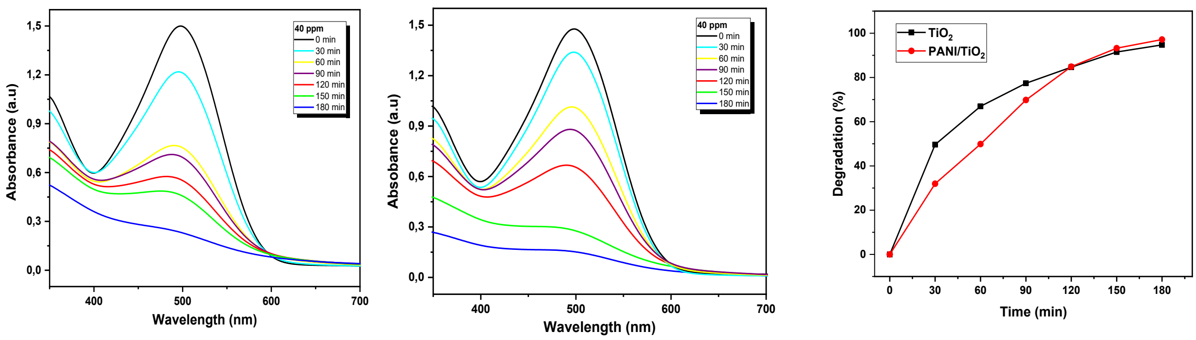

(a) (b) (c)

Figure 4 (a) - (b) Photocatalytic activity, (c) Degradation of TiO_2 and PANI/TiO_2 to CR.

Congo red (CR) is an azo dye with anionic properties soluble in water. This dye is widely used in the textile, paper, and biological product industries as a dye due to its ability to provide a bright red color to paper and fabric. However, CR is a dangerous compound because it is carcinogenic and challenging to decompose naturally. The degradation process of CR dyes, which has been widely studied, uses photocatalysts to accelerate the decomposition process of CR with the help of UV light. **Table 1** shows the research results related to the degradation of CR dyes using several materials, such as ZnO, TiO_2, and rGO. From **Table 1**, it can be seen that all degradation processes are carried out at room temperature and normal pH. With UV or visible light's help, the CR compound has been successfully decomposed into more minor compounds. Compared to several other studies, the position of this study can be seen that the level of PANI/TiO_2 degradation is higher than that of previous studies. However, it takes a longer degradation time. This longer degradation time is needed to degrade CR dyes with higher concentrations.

Table 1 Photocatalysis application of several materials on Congo Red dyes.

Materials	Source of Light	Operating conditions	Degradation Efficiency (%)	React. Time (hr)	Degradation Mechanism	Ref
TiO_2	UV	pH 7, 25 °C, CR 10 ppm	85	2	Hydroxyl radical (-OH)	[9]
ZnO	UV	pH 5, 30 °C, CR 20 ppm	78	3	Electron-hole generation	[29]
Fe-doped TiO_2	UV	pH 6, 25 °C, CR 15 ppm	92	1.5	Increased light absorption	[30]
g-C_3N_4	UV	pH 6.5, 25 °C, CR 5 ppm	70	4	Photogeneration of e-h pairs	[3]
CuO/TiO_2	Visible	pH 8, 27 °C, CR 20 ppm	90	2.5	Heterojunction electron transfer	[5]
La-CeO_2	UV	pH 7, 28 °C, CR 10 ppm	95	1	Electron-hole generation	[31]
ZnO@PANI/coal	Visible	pH 7, 28 °C, CR 5 ppm	100	1.5	Absorption of visible light	[32]
PANI/TiO_2	UV	pH 7, 28 °C, CR 40 ppm	97.12	3	Hydroxyl radical (-OH)	This study

Conclusions

This study successfully achieved the green synthesis of TiO_2 NPs using papaya leaf extract as a reducing agent. This leads to irregular spherical particles with an average size of 56 nm. The synthesis of PANI/TiO_2 NCs was conducted via the in-situ polymerization method, which was confirmed by the detection of Nitrogen (N) in EDX analysis. PANI/TiO_2 NCs exhibited a band gap energy of 2.06 eV, suggesting potential material for photocatalytic applications. The photocatalytic performance of PANI/TiO_2 NCs showed a higher degradation percentage of 97.12 % for 40 ppm CR, compared to 95.52 % for TiO_2 NPs at 40 ppm CR. The enhanced performance due to the smaller band gap of PANI/TiO2 NCs and effective charge separation facilitated the presence of PANI with TiO_2 lattice. These factors contribute to a lower recombination rate and enhanced excitation efficiency, making the photocatalytic process more effective. The degradation rate of PANI/TiO_2 for 40 ppm CR dye is better than the results of previous studies.

Acknowledgments

Thank you to the Physical Materials Laboratory, Universitas Negeri Surabaya, Indonesia which has provided facilities for making samples and photocatalytic testing, to the Institute of Life Sciences and Engineering, Airlangga University, Indonesia which has permitted test to determine the phase and morphological shape of the sample, not forgetting to DRTPM, which has funded the research, with decree number 0459/E5/PG.02.00/2024.

References

[1] Z Xu, Z Fan, C Shen, Q Meng, G Zhang and C Gao. Porous composite membrane based on organic substrate for molecular sieving: Current

status, opportunities, and challenges. *Advanced Membranes* 2022; **2**, 100027.

[2] H Kumari, Sonia, Suman, R Ranga, S Chahal, S Devi, S Sharma, S Kumar, P Kumar, S Kumar, A Kumar and R Parmar. A review on photocatalysis used for wastewater treatment: Dye degradation. *Water, Air, & Soil Pollution* 2023; **234(6)**, 349.

[3] Z Fu, H Wang, Y Wang, S Wang, Z Li and Q Sun. Construction of three-dimensional g-C3N4/Gr-CNTs/TiO2 Z-scheme catalyst with enhanced photocatalytic activity. *Applied Surface Science* 2020; **510**, 145494.

[4] V Vignesh and G Shanmugam. Removal and recovery of hazardous congo red from aqueous environment by selective natural amino acids in simple processes. *Process Biochemistry* 2023; **127**, 99-111.

[5] GA Saygılı. Synthesis, characterization and adsorption properties of a novel biomagnetic composite for the removal of congo red from aqueous medium. *Journal of Molecular Liquids* 2015; **211**, 515-526.

[6] S Singh, S Perween and A Ranjan. Journal of environmental chemical engineering dramatic enhancement in adsorption of congo red dye in polymer-nanoparticle composite of polyaniline-zinc titanate. *Journal of Environment Chemical Engineering* 2021; **9(3)**, 105149.

[7] A Rianjanu, ASP Mustamin, EKA Melati, R Aflaha, NI Khamidy, M Utami, K Khairurrijal, K Triyana, FF Abdi, HS Wasisto and T Taher. Photocatalytic degradation of aqueous congo red dye pollutants by rare-earth metal oxide (CeO_2) nanorods. *Colloids and Surfaces A: Physicochemical and Engineering Aspects* 2024; **682**, 132919.

[8] MY Chong and YJ Tam. Bioremediation of dyes using coconut parts via adsorption: A review. *SN Applied Sciences* 2020; **2**, 187.

[9] Y Yang, K Liu, F Sun, Y Liu and J Chen. Enhanced performance of photocatalytic treatment of congo red wastewater by CNTs-Ag-modified TiO_2 under visible light. *Environmental Science and Pollution Research* 2022; **29**, 15516-15525.

[10] M Tanzifi, K Karimipour, M Najafifard and S mirchenari. Removal of congo red anionic dye from aqueous solution using polyaniline/TiO_2 and polypyrrole/TiO_2 nanocomposites: Isotherm, kinetic, and thermodynamic studies. *Internation Journal of Engineering* 2016; **29(12)**, 1659-1669.

[11] H Kaur, S Kumar, S Kaushal, R Badru, PP Singh and A Pugazhendhi. Highly customized porous TiO_2-PANI nanoparticles with excellent photocatalytic efficiency for dye degradation. *Environmental Research* 2023; **225**, 114960.

[12] A Kumar, CJ Raorane, A Syed, AH Bahkali, AM Elgorban, V Raj and SC Kim. Synthesis of TiO_2, TiO_2/PAni, TiO_2/PAni/GO nanocomposites and photodegradation of anionic dyes rose bengal and thymol blue in visible light. *Environmental Research* 2023; **216(3)**, 114741.

[13] N Turkten, Y Karatas, CS Uyguner-Demirel and M Bekbolet. Preparation of PANI modified TiO_2 and characterization under pre- and post-photocatalytic conditions. *Environmental Science and Pollution Research* 2023; **30**, 111182-111207.

[14] R Khalili and H Eisazadeh. Preparation and characterization of polyaniline/Sb_2O_3 nanocomposite and its application for removal of Pb(II) from aqueous media. *International Journal of Engineering* 2013; **27(2)**, 239-246.

[15] S Zarrin and F Heshmatpour. Photocatalytic activity of TiO_2/Nb_2O_5/PANI and TiO_2/Nb_2O_5/RGO as new nanocomposites for degradation of organic pollutants. *Journal of Hazardous Materials* 2018; **351**, 147-159.

[16] U Rajaji, SEGD Rani, S Chen, K Rajakumar, M Govindasamy, FM Alzahrani, NS Alsaiari, M Ouladsmane and IS Lydia. Synergistic photocatalytic activity of SnO_2/PANI nanocomposite for the removal of direct blue 15 under UV light irradiation. *Ceramics International* 2021; **47(20)**, 29225-29231.

[17] M Mitra, ST Ahamed, A Ghosh, A Mondal, K Kargupta, S Ganguly and D Banerjee. Polyaniline/Reduced graphene oxide composite-enhanced visible-light-driven photocatalytic activity for the degradation of organic dyes. *ACS Omega* 2019; **4(1)**, 1623-1635.

[18] F Habtamu, S Berhanu and T Mender. Polyaniline supported Ag-doped ZnO nanocomposite: Synthesis, characterization, and kinetics study for photocatalytic degradation of malachite green. *Journal of Chemistry* 2021; **2021(1)**, 2451836.

[19] MM Talukder, MMR Khan and MK Amin. A review on polyaniline (PANI) based nanocomposites for water purification. *South African Journal of Chemical Engineering* 2023; **44**, 276-282.

[20] NP Putri, SR Wibowo, LN Maulida, E Suaebah, L Rohmawati, FU Ermawati and ZAI Supardi. Aplication of PANI/metal oxide composite as an active material of liquid petroleum gas sensor. *Digest Journal of Nanomaterials and Biostructures*. 2023; **18(2)**, 485-493.

[21] G Rajakumar, AA Rahuman, B Priyamvada, VG Khanna, DK Kumar and PJ Sujin. Eclipta prostrata leaf aqueous extract mediated synthesis of titanium dioxide nanoparticles. *Materials Letters* 2012; **68**, 115-117.

[22] Y Meng, Z Huang, D Liu and S Xia. Trimer cyanuramide molecular crosslinking of polyaniline mesh structures for enhanced photoelectrocatalytic water splitting efficiency. *Separation and Purification Technology* 2025; **354(8)**, 129584.

[23] I Khan, K Saeed and I Khan. Nanoparticles: Properties, applications and toxicities. *Arabian Journal of Chemistry* 2019; **12(7)**, 908-931.

[24] E Keles, M Yildirim, T Ozturk and OA Yildirim. Hydrothermally synthesized UV light active zinc stannate:tin oxide (ZTO:SnO_2) nanocomposite photocatalysts for photocatalytic applications. *Materials Science in Semiconductor Processing* 2020; **110**, 104959.

[25] SP Singh, S Kumar, SV Mathan, MS Tomar, RK Singh, PK Verma, A Kumar, S Kumar, RP Singh and AA Daru. Therapeutic application of *Carica papaya* leaf extract in the management of human diseases. *DARU Journal of Pharmaceutical Sciences* 2020; **28(2)**, 735-744.

[26] TJ Brooms, B Onyango, MS Ochieng and A Ocheieng. Photocatalytic degradation of P-cresol using TiO_2/ZnO hybrid surface capped with polyaniline. *Journal of Environmental Science and Health, Part A Toxic/Hazardous Substances and Environmental Engineering* 2018; **53(2)**, 99-107.

[27] SS Sambaza, A Maity and K Pillay. Polyaniline-Coated TiO_2 nanorods for photocatalytic degradation of bisphenol a in water. *ACS Omega* 2020; **5(46)**, 29642-29656.

[28] A Kumar and G Pandey. Comparative photocatalytic degradation of rose bengal dye under visible light by TiO_2, TiO_2/PAni and TiO_2/PAni/GO nanocomposites. *International Journal for Research in Applied Science & Engineering Technology* 2018; **6(2)**, 339-350.

[29] L Rohmawati, LR Lailia, NP Putri, M Nasir and D Darminto. Characterization of ZnO nanoparticles pineapple skin extract (Ananas comosus L.) as photocatalytic activity. *Journal of Water and Environmental Nanotechnology* 2024; **9(1)**, 112-123.

[30] Z Liu, W Zhang, X Zhao, X Sheng, Z Hu, Q Wang, Z Chen, S Wang, X Zhang and X Wang. Efficient adsorption-assisted photocatalysis degradation of congo red through loading ZIF-8 on KI-Doped TiO_2. *Materials* 2022; **15(8)**, 2857.

[31] A Rianjanu, KDP Marpaung, Siburian, SA Muhtar, NI Khamidy, J Widakdo, N Yulianto, R Aflaha, K Triyana and T Taher. Enhancement of photocatalytic activity of CeO2 nanorods through Lanthanum doping (La-CeO2) for the degradation of Congo red dye. *Result in Engineering* 2024; **23**, 102748.

[32] MA Sayed, A Mohamed, SA Ahmed, AM El-Sherbeeny, WA Zoubi and MR Abukhadra. Enhanced photocatalytic degradation of Congo red dye into safe end-products over ZnO@polyaniline/coal composite as low cost catalyst under visible light: Pathways and ecotoxicity. *Journal of Photochemistry and Photobiology A: Chemistry*. 2024; **456**, 115843.